JOC Article

Chromogenic Oxazines for Cyanide Detection

Massimiliano Tomasulo,[†] Salvatore Sortino,*[,‡] Andrew J. P. White,[§] and Françisco M. Raymo*[,†]

Center for Supramolecular Science, Department of Chemistry, University of Miami, 1301 Memorial Drive, Miami, Florida 33146-0431, Dipartimento di Scienze Chimiche, Universitá di Catania, viale Andrea Doria 8, Catania, I-95125, Italy, and Department of Chemistry, Imperial College London, South Kensington, London, SW7 2AZ, United Kingdom

ssortino@unict.it; fraymo@miami.edu

Received October 6, 2005

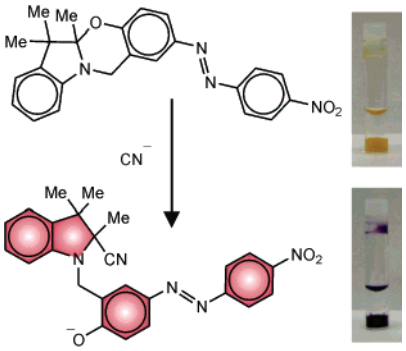

We have designed two heterocyclic compounds for the colorimetric detection of cyanide. The skeleton of both molecules fuses a benzooxazine ring to an indoline fragment and can be assembled efficiently in three synthetic steps starting from commercial precursors. The two compounds differ in the nature of the substituent on the carbon atom at the junction of the fused heterocycles, which can be either a methyl or a phenyl group. In the presence of cyanide, both molecules are converted quantitatively into cyanoamines with the concomitant appearance of an intense band in the visible region of the absorption spectrum. The developing absorption is a result of the opening of the benzooxazine ring with the formation of a 4-nitrophenylazophenolate chromophore. Nuclear magnetic resonance spectroscopy and X-ray crystallographic analyses demonstrate that the covalent attachment of a cyanide anion to the indoline fragment is responsible for these transformations. The chromogenic process is particularly fast for the methyl-substituted oxazine and can be exploited to detect micromolar concentrations of cyanide in water. Furthermore, the colorimetric response of this compound to cyanide does not suffer the interference of the halide anions, which instead are known to complicate the detection of cyanide in conventional sensing protocols. Thus, our mechanism and compounds for the colorimetric identification of cyanide can lead to the development of practical strategies for the convenient determination of this toxic anion in aqueous environments.

Introduction

The cyanide anion is a particularly strong nucleophile and forms stable complexes with a variety of transition metals in aqueous solution.[1−3] In fact, a wealth of diverse industrial applications have been developed around the excellent binding properties of this particular ligand.[4,5] The strong affinity of

[†] University of Miami.
[‡] Universitá di Catania.
[§] Imperial College London.

(1) Dunbar, K. R.; Heintz, R. A. *Prog. Inorg. Chem.* **1997**, *45*, 283−391.
(2) Verdaguer, M.; Bleuzen, A.; Marvaud, V.; Vaissermann, J.; Seuleiman, M.; Desplanches, C.; Scuiller, A.; Train, C.; Garde, R.; Gelly, G.; Lomenech, C.; Rosenman, I.; Veillet, P.; Cartier, C.; Villain, F. *Coord. Chem. Rev.* **1999**, *192*, 1023−1047.
(3) Baraldo, L. M.; Forlano, P.; Parise, A. R.; Slep, L. D.; Olabe, J. A. *Coord. Chem. Rev.* **2001**, *219*, 881−921.
(4) Young, C.; Tidwell, L.; Anderson, C. *Cyanide*: *Social, Industrial, and Economic Aspects*; Minerals, Metals, and Materials Society: Warrendale, 2001.

10.1021/jo052096r CCC: $33.50
Published on Web 12/09/2005

cyanide for transition metals, however, has deleterious consequences on cell metabolism.[6−8] Specifically, this anion binds the active site of cytochrome oxidase and inhibits the mitochondrial electron-transport chain. As a result, cyanide is extremely toxic and even relatively small amounts of this species (0.5−3.5 mg per kg of body weight) are lethal to humans.[9] Unfortunately, cyanide does not easily decompose in the environment.[10] Therefore, the accidental spillage of this toxic chemical from industrial plants, or even its intentional release, can contaminate drinking waters and become a serious threat to human health. Indeed, the concentration of cyanide in drinking water cannot be greater than 1.9 μM according to the World Health Organization.[11]

Numerous standard methods for the detection of micromolar amounts cyanide in water have been developed relying on a diversity of experimental protocols and detection techniques.[12] Most of these strategies, however, require either multistep procedures with tedious sample pretreatments or sophisticated instrumentation. The development of chemosensors[13−16] for the recognition of anions[17−31] can facilitate the qualitative, and perhaps even the quantitative, determination of cyanide. In particular, the identification of chromogenic compounds that respond to the presence of cyanide anions with fast and visible color changes would offer the opportunity to screen rapidly water samples relying exclusively on the naked eye. Indeed, few organic molecules and transition metal complexes able to signal the presence of cyanide with pronounced changes in their absorption and emission properties have been already identified.[32−37] Their operating principles are based on hydrogen bonding interactions, metal coordination, or the formation of covalent bonds between the nucleophilic cyanide anion and compatible electrophilic centers. Some of these chemosensors can even detect micromolar amounts of cyanide;[36,37] however, most of them suffer the deleterious interference of other anions.[32−37] Halide anions in particular, and especially fluoride, tend to mask the response of cyanide.[32,34b,35,37c] In search for specific chemosensors for the colorimetric determination of cyanide, we have designed a series of chromogenic oxazines. In this article, we illustrate the logic behind our molecular design and we report the synthesis and characterization of these compounds together with their colorimetric response to cyanide.

Results and Discussion

Design and Synthesis. Recently, we have discovered that the [1,3]oxazine **1a** (Figure 1) is converted quantitatively into the hemiaminal **1c** upon treatment with Bu_4NOH in acetonitrile.[38] The nucleophilic attack of the hydroxide anion of Bu_4NOH to the indolium cation of the short-lived intermediate **1b** is responsible for this transformation. Interestingly, the bimolecular conversion of **1a** into **1c** is accompanied by the appearance of a yellowish color. Indeed, the absorption spectrum of **1a** shows bands in the ultraviolet region only, while the 4-nitrophenolate chromophore of **1c** has an intense absorption centered at 440 nm.

On the basis of these observations, we have tested the response of **1a** to Bu_4NCN under otherwise identical conditions. Once again, the characteristic band of a 4-nitrophenolate chromophore appears in the visible region of the absorption

(5) *Ullmann's Encyclopedia of Industrial Chemistry*; Wiley-VCH: New York, 2003.
(6) Vennesland, B. *Cyanide in Biology*; Academic Press: New York, 1981.
(7) Kulig, K. W. *Cyanide Toxicity*; U.S. Department of Health and Human Services: Atlanta, GA, 1991.
(8) Baskin, S. I.; Brewer, T. G. In *Medical Aspects of Chemical and Biological Warfare*; Sidell, F. R., Takafuji, E. T., Franz, D. R., Eds.; TMM Publications: Washington, DC, 1997; pp 271−286.
(9) Muir, G. D. *Hazards in the Chemical Laboratory*; The Royal Chemical Society: London, UK, 1977.
(10) Baird, C.; Cann, M. *Environmental Chemistry*; Freeman: New York, 2005.
(11) *Guidelines for Drinking-Water Quality*; World Health Organization: Geneva, Switzerland, 1996.
(12) Ikebukuro, K.; Nakamusa, H.; Karude, I. In *Handbook of Water Analysis*; Nollet, L. M., Ed.; Marcel Dekker: New York, 2000; Vol. 102, pp 367−385.
(13) Desvergne, J.-P.; Czarnik, A. W., Eds. *Chemosensors of Ion and Molecular Recognition*; Kluwer Academic Publishers: Dordrecht, The Netherlands, 1997.
(14) Ricco, A. J.; Crooks, R. M., Eds. Chemical Sensors. *Acc. Chem. Res.* **1998**, *31*, 199−324.
(15) Ellis, A. B.; Walt, D. R., Eds. Chemical Sensors. *Chem. Rev.* **2000**, *100*, 2477−2738.
(16) Fabbrizzi, L., Ed. Luminescent Sensors. *Coord. Chem. Rev.* **2000**, *205*, 1−232.
(17) Bianchi, A.; Bowman-James, K.; Garcia-España, E., Eds. *Supramolecular Chemistry of Anions*; Wiley-VCH: New York, 1997.
(18) Gale, P. A., Ed. 35 Years of Synthetic Anion Receptor Chemistry 1968−2003. *Coord. Chem. Rev.* **2003**, *240*, 1−226.
(19) (a) Schmidtchen, F. P.; Gleich, A.; Schummer, A. *Pure Appl. Chem.* **1989**, *61*, 1535−1546. (b) Schmidtchen, F. P.; Berger, M. *Chem. Rev.* **1997**, *97*, 1609−1646.
(20) Dietrich, B. *Pure Appl. Chem.* **1993**, *65*, 1457−1464.
(21) Czarnik, A. W. *Acc. Chem. Res.* **1994**, *27*, 302−308.
(22) Atwood, J. L.; Holman, K. T.; Steed, J. W. *Chem. Commun.* **1996**, 1401−1407.
(23) (a) Scheerder, J.; Engbersen, J. F. J.; Reinhoudt, D. N. *Recl. Trav. Chim. Pays-Bas* **1996**, *115*, 307−320. (b) Antonisse, M. M. G.; Reinhoudt, D. N. *Chem. Commun.* **1998**, 443−448.
(24) (a) Beer, P. D.; Smith, D. K. *Prog. Inorg. Chem.* **1997**, *46*, 1−96. (b) Beer, A. D. *Acc. Chem. Res.* **1998**, *31*, 71−80. (c) Beer, P. D.; Gale, P. A.; Chen, G. Z. *Coord. Chem. Rev.* **1999**, *186*, 3−36. (d) Beer, P. D.; Gale, P. A. *Angew. Chem., Int. Ed.* **2001**, *40*, 487−516.
(25) (a) de Silva, A. P.; Gunaratne, H. Q. N.; Gunnlaugsson, T.; Huxley, A. J. M.; McCoy, C. P.; Rademacher, J. T.; Rice, T. E. *Chem. Rev.* **1997**, *97*, 1515−1566. (b) de Silva, A. P.; Fox, D. B.; Huxley, A. J. M.; McClenaghan, N. D.; Roiron, J. *Coord. Chem. Rev.* **1999**, *186*, 297−306.
(26) (a) Gale, P. A.; Sessler, J. L.; Kral, V. *Chem. Commun.* **1998**, 1−8. (b) Sessler, J. L.; Anzenbacher, P., Jr.; Jursikova, K.; Miyaji, H.; Genge, J. W.; Tvermoes, N. A.; Allen, W. E.; Shriver, J. A.; Gale, P. A.; Kral, V. *Pure Appl. Chem.* **1998**, *70*, 2401−2408. (c) Gale, P. A.; Anzenbacher, P., Jr.; Sessler, J. L. *Coord. Chem. Rev.* **2001**, *222*, 57−102.
(27) (a) Gale, P. A. *Coord. Chem. Rev.* **2000**, *199*, 181−233. (b) Gale, P. A. *Coord. Chem. Rev.* **2001**, *213*, 79−128.
(28) (a) Wiskur, S. L.; Ait-Haddou, H.; Lavigne, J. J.; Anslyn, E. V. *Acc. Chem. Res.* **2001**, *34*, 963−972. (b) Lavigne, J. J.; Anslyn, E. V. *Angew. Chem., Int. Ed.* **2001**, *40*, 3119−3130.
(29) Amendola, V.; Fabbrizzi, L.; Mangano, C.; Pallavicini, P.; Poggi, A.; Taglietti, A. *Coord. Chem. Rev.* **2001**, *219*, 821−837.
(30) Martínez-Máñez, R.; Sancerón, F. *Chem. Rev.* **2003**, *103*, 4419−4476.
(31) Suksai, C.; Tuntulani, T. *Chem. Soc. Rev.* **2003**, *32*, 192−202.
(32) Miyaji, H.; Sessler, J. L. *Angew. Chem., Int. Ed.* **2001**, *40*, 154−157
(33) Kim, Y.-H.; Hong, J.-I. *Chem. Commun.* **2002**, 512−513.
(34) (a) Ros-Lis, J. V.; Martínez-Máñez, R.; Soto, J. *Chem. Commun.* **2002**, 2248−2249. (b) Jiménez, D.; Martínez-Máñez, R.; Sancenón, F.; Soto, J. *Tetrahedron Lett.* **2002**, *43*, 2823−2825.
(35) (a) Anzenbacher, P., Jr.; Tyson, D. S.; Jursíková, K.; Castellano, F. N. *J. Am Chem. Soc.* **2002**, *124*, 6232−6233. (b) Anzenbacher, P., Jr.; Jursíková, K.; Aldakov, D.; Marquez, M.; Pohl, R. *Tetrahedron* **2004**, *60*, 11163−11168.
(36) Chow, C.-F.; Lam, M. H. W.; Wong, W.-Y. *Inorg. Chem.* **2004**, *43*, 8387−8393.
(37) (a) Badugu, R.; Lakowicz, J. R.; Geddes, C. D. *Anal. Chim. Acta* **2004**, *522*, 9−17. (b) Badugu, R.; Lakowicz, J. R.; Geddes, C. D. *Dyes Pigmen.* **2005**, *64*, 49−55. (c) Badugu, R.; Lakowicz, J. R.; Geddes, C. D. *J. Am. Chem. Soc.* **2005**, *127*, 3635−3641.
(38) (a) Tomasulo, M.; Sortino, S.; Raymo, F. M. *Org. Lett.* **2005**, *7*, 1109−1112. (b) Tomasulo, M.; Sortino, S.; White, A. J. P.; Raymo, F. M. *J. Org. Chem.* **2005**, *70*, 8180−8189.

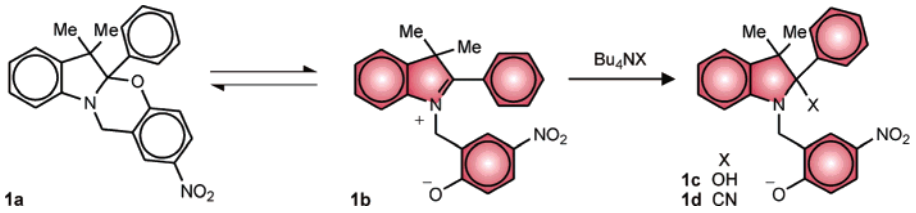

FIGURE 1. Transformation of the [1,3]oxazine **1a** into either the hemiaminal **1c** or the cyanoamine **1d**.

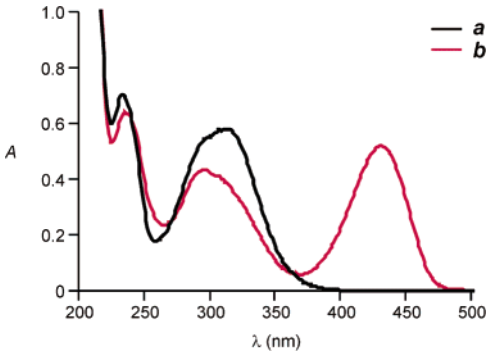

FIGURE 2. Steady-state absorption spectra (0.1 mM, MeCN, 298 K) of **1a** before (a) and after (b) the addition of Bu_4NCN (100 equiv).

spectrum (a and b in Figure 2) after the addition of the nucleophile. Thus, the cyanide anion can also react with the intermediate **1b** and trap its 4-nitrophenolate chromophore in the form of the cyanoamine **1d** (Figure 1) with the concomitant appearance of color. It follows that similar transformations can be a possible operating mechanism for the colorimetric detection of cyanide. In this context, we have designed the two compounds **7a** and **8a** (Figure 3). They share a central [1,3]oxazine ring with **1a**, but incorporate a 4-nitrophenylazo appendage in place of the nitro group. After ring opening and nucleophilic trapping, the extended conjugation of the resulting 4-nitrophenylazophenolate chromophore should translate into an enhancement of ca. 18 mM^{-1} cm^{-1} in molar extinction coefficient, relative to the 4-nitrophenolate chromophore of **1c**. Thus, **7a** and **8a** should be more appropriate than **1a** as potential chromogenic probes for cyanide.

We have synthesized the two [1,3]oxazines **7a** and **8a** in two steps (Figure 3) starting from 2-hydroxymethylphenol (**2**) and 4-nitrobenzenediazonium tetrafluoroborate (**3**).[39] The reaction of **2** and **3** in aqueous NaOH affords the 4-nitrophenylazophenol **4** in a yield of 96%. The treatment of **4** with PBr_3 and the reaction of the resulting bromide with an excess of the indole **5** or **6** in situ gives the corresponding [1,3]oxazine **7a** or **8a** in a yield of 41% or 51%, respectively.

X-ray Crystallography. The X-ray analysis of crystals of the cyanoamine **1d** confirmed the opening of the benzooxazine ring with the addition of a cyano group (Figure 4). The structure is somewhat similar to that of the hemiaminal **1c**,[38b] including the incorporation of water molecules hydrogen bonded to the phenolate anion. The indoline ring of **1d** has an envelope-type geometry, C(9) lying ca. 0.46 Å out of the {N(1) to C(8)} plane, which is coplanar to within ca. 0.02 Å. The geometry at N(1) is similar to those seen in related species,[38b] the nitrogen center being pyramidal (ca. 0.33 Å out of the plane of its substituents), and with its $2p_z$ orbital approximately collinear with the σ orbital

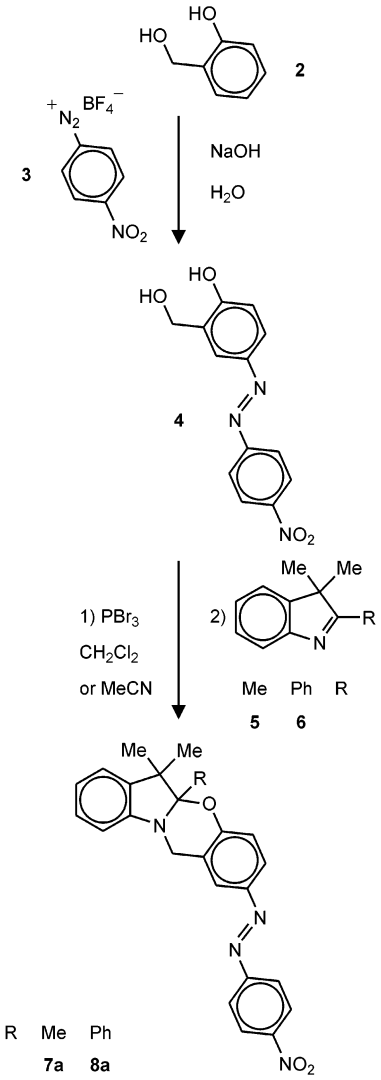

FIGURE 3. Synthesis of the [1,3]oxazines **7a** and **8a**.

of the C(9)−C(20) bond [the C(20)−C(9)−N(1)−lone pair dihedral angle is ca. 13°].

As can readily be seen from Figure 4, the packing in the crystals of **1d** is dominated by O−H···O hydrogen bonds involving the phenolate anion and the three included water molecules. There are also, however, some notable cation···anion contacts with both rings **A** and **B** approached by methylene protons from the tetra-*n*-butylammonium cation [H···**A** 2.95 Å, C−H···**A** 178°; H···**B** 2.78 Å, C−H···**B** 175°]. The opposite faces of both of these rings are involved in a bifurcated C−H···π hydrogen bond from a methyl proton of the cation [H···**A** 3.28 Å, C−H···**A** 119°; H···**B** 3.15 Å, C−H···**B** 129°], the angles subtended at each ring centroid being ca. 155 and 172° for **A**

(39) Tomasulo, M.; Raymo, F. M. *Org. Lett.* **2005**, *7*, 4633−4636.

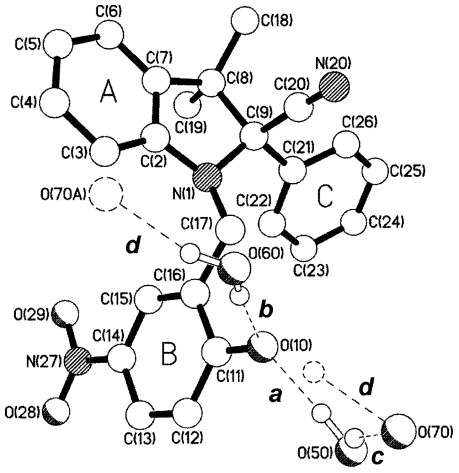

FIGURE 4. The single-crystal X-ray structure of **1d** (cation not depicted) showing the O−H···O hydrogen bonding interactions between the phenolate anion and the included solvent water molecules. The O−H···O hydrogen bonding geometries, [O···O] (Å), [H···O] (Å), and [O−H···O] (deg), are the following: (a) 2.718(4), 1.83, 167; (b) 2.719(4), 1.83, 172; (c) 2.771(5), 1.92, 158; (d) 2.742(5), 1.87, 163.

and **B**, respectively. Ring **C** is not involved in any noteworthy intermolecular contacts.

The X-ray analysis of crystals of **7a** revealed the presence of two independent molecules, **I** and **II** (see Figures 5 and S5 for pictures of molecules **I** and **II**, respectively). With the exception of the terminal *p*-nitrophenyl substituents, the two molecules have very similar conformations (Figure S7), the N(1) to N(22) portions of the two independent molecules having a root-mean-square fit of ca. 0.048 Å. In common with **1a**,[38b] both independent molecules have the expected near orthogonal relationship between their indoline and benzooxazine ring systems (ca. 86° in both molecules). The indoline ring in each independent molecule has a similar envelope-type geometry to that seen in **1a** [in **I** C(9) is ca. 0.46 Å out of the {N(1) to C(8)} plane, which is coplanar to within ca. 0.04 Å; in **II** C(9′) is ca. 0.51 Å out of the {N(1′) to C(8′)} plane, which is coplanar to within ca. 0.02 Å]. By contrast, the benzooxazine rings are more distorted. In **1a**, the ring had an envelope-type geometry with N(1) lying ca. 0.53 Å out of the plane of the remaining C_8O atoms, which were coplanar to within ca. 0.08 Å. In **7a**, however, both independent molecules have twisted benzooxazine rings with, for **I**, N(1) lying ca. 0.50 Å "below" and C(9) ca. 0.22 Å "above" the plane of the remaining C_7O atoms, which are coplanar to within ca. 0.08 Å (for **II** the values are 0.42, 0.30, and 0.06 Å, respectively).[40] In each independent molecule, the N(1) nitrogen centers have pyramidal geometries, the nitrogen lying ca. 0.36 Å out of the plane of its substituents in both **I** and **II**. As was seen in **1a**, here in both independent molecules of **7a** the nitrogen $2p_z$ orbital is approximately collinear with the σ orbital of the C(9)−O(10) bond, the O(10)−C(9)−N(1)−lone pair dihedral angles being ca. 8° and 7° in **I** and **II**, respectively. Though flat (with {C(14),N(21),N(22),-C(23)} being coplanar to within 0.01 Å [0.01 Å]), the plane of the N_2 moiety is twisted with respect to ring **B** by ca. 16° [18°], and to ring **C** by ca. 29° [21°]; these twists are in the same sense so that ring **C** is twisted by ca. 46° [39°] with respect to ring **B** [the values for molecule **II** are given in square brackets]. The terminal nitro group is rotated by ca. 16° [10°] to ring **C**.

Adjacent molecules are linked by C−H···π interactions; ring **A** (in molecule **I**) is approached by a C(4′)−H proton from molecule **II** [H···**A** 2.45 Å, C(4′)−H···**A** 176°], ring **B** in molecule **I** is approached by a C(20)−H proton in a neighboring molecule **I** [H···**B** 2.91 Å, C(20)−H···**B** 145°], and similarly ring **B′** in molecule **II** is approached by a C(20′)−H proton from another molecule **II** [H···**B** 2.82 Å, C(20′)−H···**B** 153°]. There is also some evidence for a possible weak O···π interaction between the nitro group of molecule **II** and ring **C** in molecule **I** with an O(30′)···**C** separation of ca. 3.22 Å.

The single-crystal structure of **8a** (the phenyl analogue of **7a**) is similar, though here there is only one independent molecule, and the azo-4-nitrophenyl moiety adopts a noticeably different conformation (Figure 7) where the azo unit is anti with respect to the C(17) carbon center (in both independent molecules of **7a** the relationship was gauche). The fused indoline/benzooxazine core of the structure is very similar to that seen in **7a**. The indoline ring adopts an envelope-type geometry with C(9) lying ca. 0.47 Å out of the C_7N plane (which is coplanar to within ca. 0.05 Å), while the benzooxazine ring again has a twisted conformation with N(1) ca. 0.35 Å "below" and C(9) ca. 0.28 Å "above" the C_7O plane (which is coplanar to within ca. 0.03 Å); the C_7N and C_7O planes are inclined by ca. 80°. The N(1) is again pyramidal, lying ca. 0.36 Å out of the plane of its substituents, and the nitrogen $2p_z$ orbital is approximately collinear with the σ orbital of the C(9)−O(10) bond, the O(10)−C(9)−N(1)−lone pair dihedral angle being ca. 8°. The C−N═N−C unit is again flat (coplanar to better than 0.01 Å), but unlike in **7a**, here it is almost coplanar with both ring **B** (rotated by ca. 6°) and ring **C** (rotated by ca. 1°). The terminal nitro group is rotated by ca. 10° to ring **C**.

The extended structure of **8a** is dominated by the stacking of the 4-nitrophenylazophenolate units of adjacent, centrosymmetrically related molecules linked by a combination of interactions/contacts (Figure S9). Ring **C** of one molecule lays above the azo unit of a C_i related counterpart, and vice versa, with a centroid···centroid separation of ca. 3.40 Å (a in Figure S9). In the same centrosymmetric pair, ring **B** of one molecule overlays the nitro unit of the other, the closest approach being from O(35) at ca. 3.13 Å to the ring **B** centroid (b in Figure S9). This same oxygen atom also approaches the centroid of ring **D** in the second molecule, but only at ca. 3.63 Å (c in Figure S9). These centrosymmetric pairs of molecules are linked to adjacent pairs across an independent center of symmetry by a couple of C−H···π hydrogen bonds from a nitrophenyl hydrogen atom [on C(30)] to the centroid of ring **A** [H···**A** 2.88 Å, C(30)−H···**A** 151°, d in Figure S9].

^{1}H NMR Spectroscopy. The chiral center at the junction of the two heterocycles in **7a** and **8a** imposes two distinct environments on the adjacent pairs of methyl groups (Me$^{\bigcirc}$ and Me$^{\square}$ in Figures 7 and S10) and methylene protons (H$^{\bigcirc}$ and H$^{\square}$). As a result, the ^{1}H NMR spectra of both compounds show two distinct singlets for the protons of Me$^{\bigcirc}$ and Me$^{\square}$ and an AB system for H$^{\bigcirc}$ and H$^{\square}$, when recorded in acetonitrile-d_3 at 275 K (a in Figures 7 and S10). Upon warming the solution, these resonances broaden considerably for both compounds (b and c in Figures 7 and S10) and, eventually, coalesce into single peaks for **7a** (d in Figures 7 and S10). These changes are a consequence of the interconversion between the two enantiomers of each compound on the ^{1}H NMR time scale. This process

(40) If the benzooxazine ring in **1a** is viewed as twisted in a similar fashion, then N(1) lies ca. 0.48 Å "below" and C(9) ca. 0.14 Å "above" the plane of the remaining C_7O atoms which are coplanar to within ca. 0.04 Å.

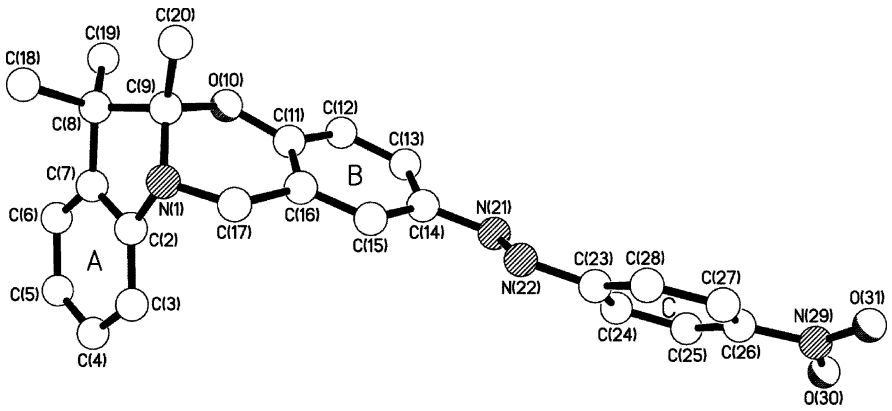

FIGURE 5. The structure of one (**I**) of the two crystallographically independent molecules present in the crystals of **7a**.

TABLE 1. Kinetic Parameters Associated with the Ring Opening of 7a and 8a at 298 K[a]

solvent	compd	k (s^{-1})	$\Delta G^{\ddagger}$ (kcal mol^{-1})	$\Delta H^{\ddagger}$ (kcal mol^{-1})	$-\Delta S^{\ddagger}$ (kcal mol^{-1} K^{-1})
acetonitrile-d_3	**7a**	25 ± 2	15.54 ± 0.04	15.0 ± 0.2	0.002 ± 0.001
	8a	0.10 ± 0.02	18.82 ± 0.11	18.5 ± 0.9	0.001 ± 0.003
toluene-d_8[b]	**7a**	0.011 ± 0.004	20.17 ± 0.23	21.4 ± 1.3	-0.004 ± 0.004

[a] The rate constant (k), free energy ($\Delta G^{\ddagger}$), enthalpy ($\Delta H^{\ddagger}$), and entropy ($\Delta S^{\ddagger}$) of activation were determined by variable-temperature ^{1}H NMR spectroscopy (ref 41). [b] In toluene-d_8, the line widths of the singlets associated with the pair of methyl protons of **8a** remain approximately constant in the examined temperature range (275−363 K). As a result, the kinetic parameters for the ring opening of this compound could not be determined.

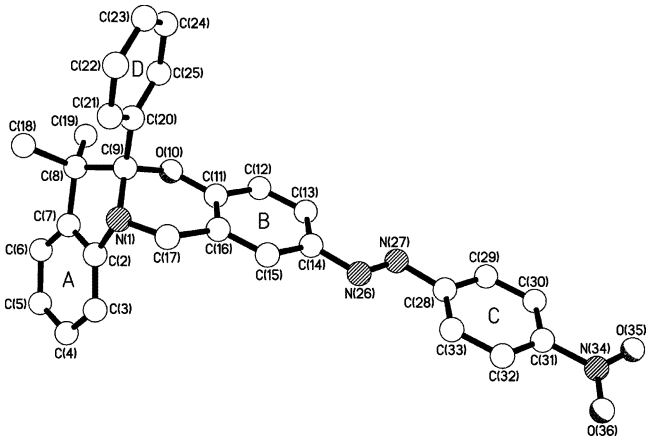

FIGURE 6. The single-crystal X-ray structure of **8a**.

involves the thermal opening of the [1,3]oxazine ring with the formation of **7b** and **8b** and their re-isomerization to **7a** and **8a**, respectively. The kinetic parameters (Table 1) associated with the ring-opening step can be extracted from the analysis of the temperature dependence of the line widths associated with the singlets for the protons of Me$^{\bigcirc}$ and Me$^{\square}$ in the slow-exchange regime.[41] In acetonitrile-d_3, the rate constants (k) are ca. 25 and 0.1 s^{-1} for **7a** and **8a**, respectively. These values correspond to free energy barriers ($\Delta G^{\ddagger}$) of ca. 16 and 19 kcal mol^{-1}, respectively. Interestingly, the $\Delta G^{\ddagger}$ values are dominated by their enthalpic terms ($\Delta H^{\ddagger}$), while the entropic contributions are negligible ($\Delta S^{\ddagger}$). In toluene-d_8, the ring-opening process is significantly slower. The k value for **7a** decreases by 4 orders of magnitude with a concomitant increase of ca. 4.5 kcal mol^{-1} in $\Delta G^{\ddagger}$. In the case of **8a**, the process is so slow that the ^{1}H NMR spectrum remains virtually unchanged over a broad range of temperatures.

The quantitative transformation of **1a** into **1c** (Figure 1) causes drastic changes in the ^{1}H NMR spectrum.[38] The two oxazines **7a** and **8a** show essentially the same behavior. Their treatment with Bu_4NOH results in the formation of the corresponding hemiaminals **7c** and **8c** (Figures S11 and S12). In both instances, the chemical shift of the diastereotopic methylene protons decreases, but their AB system is maintained, confirming the presence of a chiral center in **7c** and **8c**. A second product is also formed in the case of **7**. Indeed, the methyl group on its chiral center is relatively acidic and is partially deprotonated upon treatment with Bu_4NOH to form **7d** (Figure S11). The ratio between **7c** and **7d** can be estimated to be 70:30 from the integrals of the resonances associated with the methylene protons. The formation of the two hemiaminals **7c** and **8c** is further confirmed by the appearance of peaks at m/z 431 and 493 in the corresponding fast atom bombardment mass spectra.

The changes imposed on the ^{1}H NMR spectra of **7a** and **8a** by the addition of Bu_4NOH can be replicated with Bu_4NCN. In both instances, the cyanide anion attacks the indolium cations of **7b** and **8b** to form quantitatively **7e** and **8d**, respectively (Figures 8 and S13). As a result of these transformations, the chemical shifts of most aromatic protons decrease (a and b in Figures 8 and S13). For both compounds, the largest change (−0.45 ppm for **7a** and −0.61 ppm for **8a**) is observed for the proton in the ortho position relative to the phenolate oxygen

(41) Below the coalescence temperature, two well-separated singlets can be observed for the protons of Me$^{\bigcirc}$ and Me$^{\square}$ in the ^{1}H NMR spectra (a−c in Figures 7 and S10). Under these conditions, the line width ($\Delta\nu$) of either one of the two singlets is related to the rate constant (k) of the degenerate site-exchange process according to eq 1, where $\Delta\nu_0$ is the line width at the stopped-exchange limit (Nelson, J. H. *Nuclear Magnetic Resonance Spectroscopy*; Prentice Hall: Upper Saddle River, NJ, 2003). Following this protocol, k can be determined at any temperature (T) within the slow-exchange regime. A plot of $\ln(k\,T^{-1})$ against T^{-1} can then be fitted to eq 2, where R is the gas constant, to extract the enthalpy ($\Delta H^{\ddagger}$) and entropy ($\Delta S^{\ddagger}$) of activation. Finally, the free energy ($\Delta G^{\ddagger}$) of activation can be calculated at any T by using eq 3.

$$k = \pi(\Delta\nu - \Delta\nu_0) \quad (1)$$

$$\ln\frac{k}{T} = -\frac{\Delta H^{\ddagger}}{RT} + \frac{\Delta S^{\ddagger}}{R} + 23.76 \quad (2)$$

$$\Delta G^{\ddagger} = \Delta H^{\ddagger} - T\Delta S^{\ddagger} \quad (3)$$

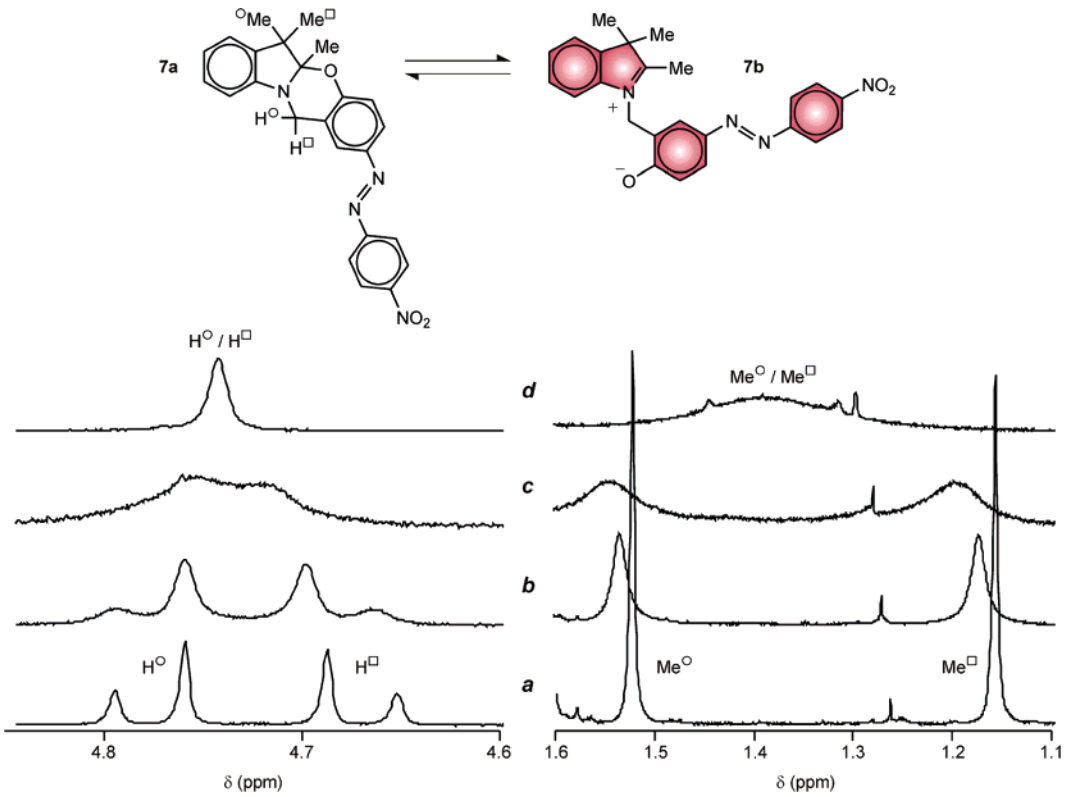

FIGURE 7. Partial ^{1}H NMR spectra (500 MHz, acetonitrile-d_3, 5 mM) of **7a** at 275 (a), 300 (b), 310 (c) and 346 K (d).

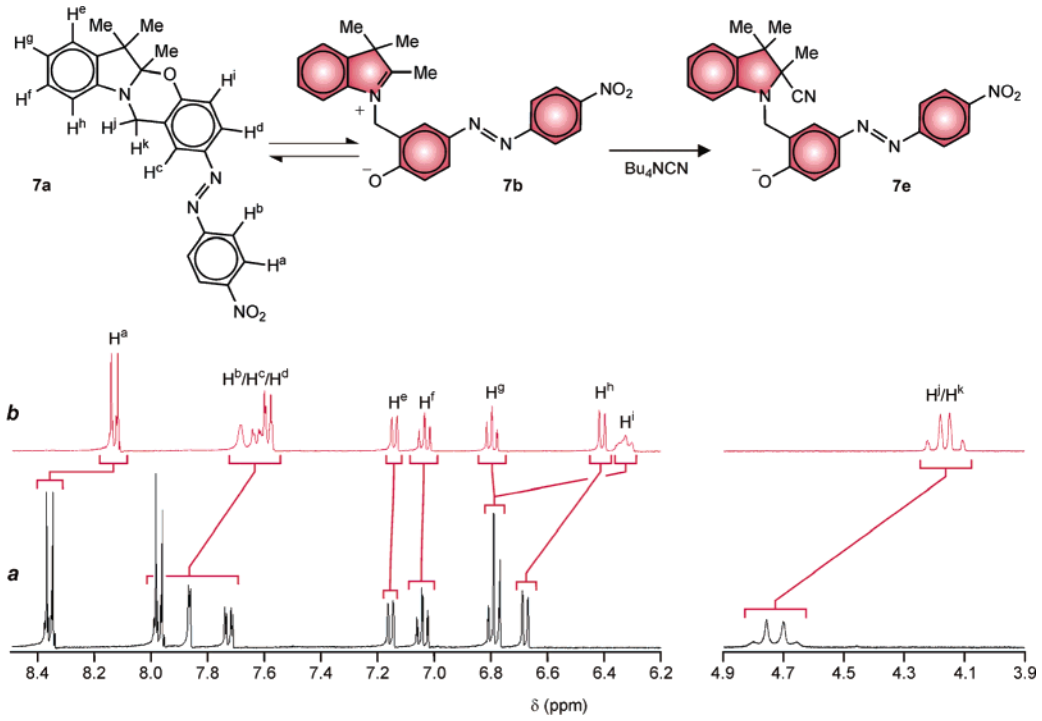

FIGURE 8. Partial ^{1}H NMR spectra (400 MHz, acetonitrile-d_3, 10 mM) of **7a** before (a) and after (b) the addition of Bu_4NCN (10 equiv).

atom (H^i for **7a** and H^l for **8a**). Once again, the AB system for the methylene protons is maintained with the transformation of **7a** into **7e** and of **8a** into **8d**, but moves by −0.57 ppm for **7** and −0.69 ppm for **8**. Furthermore, the fast atom bombardment mass spectra show the appearance of peaks at *m*/*z* 441 and 503 in support of the formation of **7e** and **8d**, respectively.

Steady-State Absorption Spectroscopy. The steady-state absorption spectra of the two [1,3]oxazines **7a** and **8a** (a in Figures 9 and S14) resemble the sum of those of the model compounds **9** or **10** (b in Figures 9 and S14) and **11** (c in Figures 9 and S14). In particular, an intense band for the $\pi \rightarrow \pi^*$ transition of the 4-nitrophenylazophenyl chromophore is evident

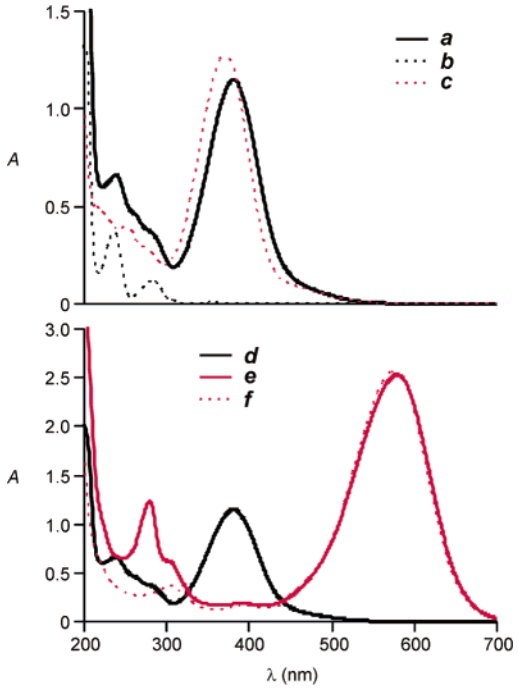

FIGURE 9. Steady-state absorption spectra (0.1 mM, MeCN, 298 K) of **7a** (a), **9** (b), **11** (c), **7a** before (d) and after (e) the addition of Bu_4NOH (1 equiv), and **12** (f).

TABLE 2. Absorption Wavelengths (λ) and Molar Extinction Coefficients (ϵ) of the Oxazines 7a and 8a and of the Model Compounds 9−12 in MeCN at 298 K[a]

compd	λ (nm)	ϵ (mM^{-1} cm^{-1})
7a	380	23.0 ± 1.2
8a	371	22.0 ± 1.1
9	283	2.2 ± 0.1
10	281	3.9 ± 0.2
11	371	26.1 ± 1.3
12	576	50.4 ± 1.1

[a] The model compounds are shown in the following diagram. The λ and ϵ of the phenolate **12** were determined by recording the absorption spectrum of the corresponding phenol in the presence of Bu_4NOH (4 equiv).

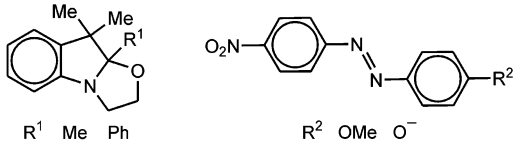

at 380 nm for **7a** and at 371 nm for **8a** (Table 2). Upon addition of Bu_4NOH, this absorption disappears with the concomitant appearance of a band at ca. 575 nm (d and e in Figures 9 and S14) for the 4-nitrophenylazophenolate chromophores of **7c**/**7d** and **8c**. Indeed, the spectrum of the model 4-nitrophenylazophenolate **12** (f in Figures 9 and S14) shows an absorption at 576 nm with a molar extinction coefficient close to 50 mM^{-1} cm^{-1} (Table 2).

The addition of Bu_4NCN to acetonitrile solutions of **7a** and **8a** causes similar absorption changes (a and b in Figures 10 and S15). Once again, the characteristic absorption of a 4-nitrophenylazophenolate chromophore can be observed at ca. 580 nm only in the presence of the nucleophile. The chromogenic transformation of **7a**, however, is significantly faster than that of **8a**. The 4-nitrophenylazophenolate absorbance of the product reaches a stationary value in less than 1 min after the addition of only 1.5 equiv of Bu_4NCN to **7a** (c in Figure 10). Instead, more than 30 min are required to complete the transformation of **8a** even in the presence of up to 15 equiv of Bu_4NCN (d in Figure 10). These observations are in full agreement with the kinetic parameters (Table 1) determined for the ring opening of **7a** and **8a** by ^1H NMR spectroscopy. Indeed, these data show that the ring opening of **8a** is 2 orders of magnitude slower than that of **7a**.

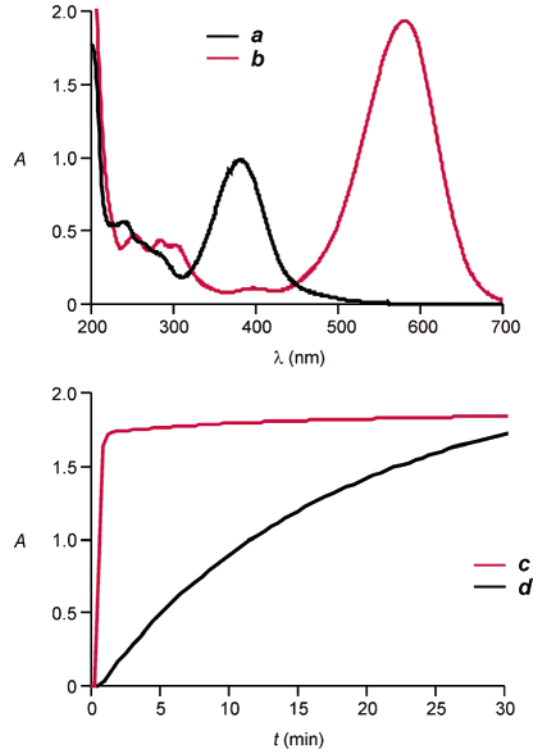

FIGURE 10. Steady-state absorption spectra (0.1 mM, MeCN, 298 K) of **7a** before (a) and after (b) the addition of Bu_4NCN (15 equiv). Evolution of the absorbance at 581 nm for solutions (0.1 mM, MeCN, 298 K) of **7a** (c) and **8a** (d) after the addition of Bu_4NCN (1.5 equiv for **7a** and 15 equiv for **8a**).

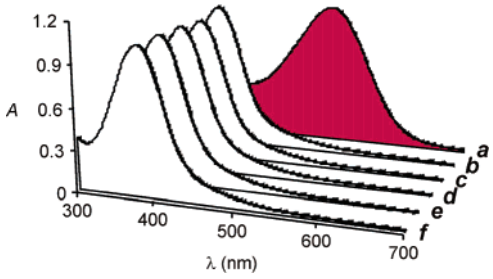

FIGURE 11. Steady-state absorption spectra (0.1 mM, 550 μL, MeCN, 298 K) of **7a** after the addition of sodium phosphate buffer (550 μL, pH 7.6) without (b) or with 10 mM of NaCN (a), NaF (c), NaCl (d), NaBr (e), or NaI (f).

The relatively fast colorimetric response of **7a** to cyanide can be exploited to sense this particular anion in aqueous environments. In fact, the addition of NaCN in sodium phosphate buffer (pH 7.6) to an acetonitrile solution of **7a** results in the appearance of the 4-nitrophenylazophenolate absorption (a in Figure 11). This band cannot be observed if the acetonitrile solution of **7a** is treated with sodium phosphate buffer lacking NaCN (b in Figure 11). Similarly, halide salts have essentially no influence on **7a** under otherwise identical conditions. Indeed,

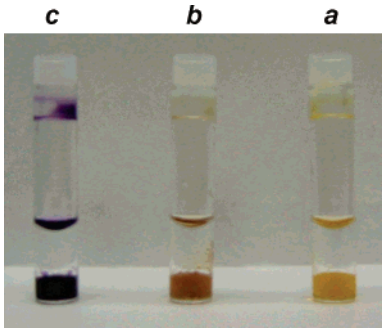

FIGURE 12. Solutions of **7a** (1 mM, 200 μL, dichloroethane, 298 K) and Bu_4NCl (1 M) with overlaid sodium phosphate buffer (500 μL, pH 9.0) without (a) or with 10 (b) or 100 μM (c) of NaCN.

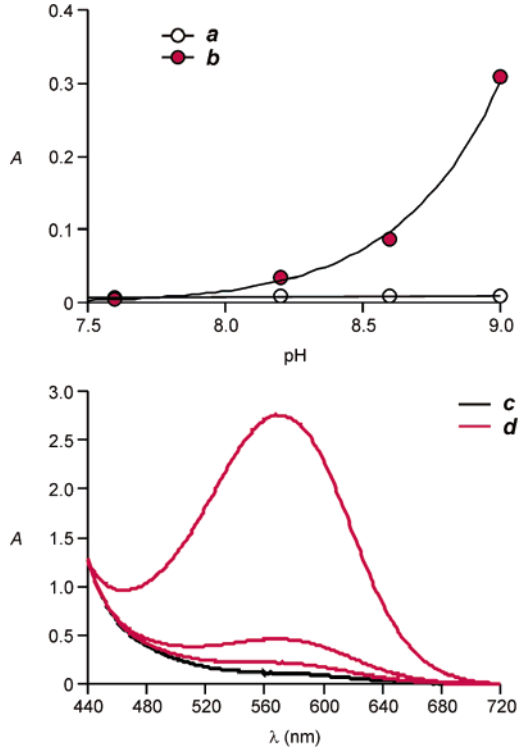

FIGURE 13. Absorbance at 581 nm of a solution of **7a** (1 mM, 200 μL, dichloroethane, 298 K) and Bu_4NCl (1 M) after treatment with sodium phosphate buffer (300 μL) without (a) or with (b) NaCN (0.1 mM) and dilution with dichloroethane (470 μL). Steady-state absorption spectra of a solution of **7a** (1 mM, 200 μL, dichloroethane, 298 K) and Bu_4NCl (1 M) after treatment with sodium phosphate buffer (100 μL, pH 9.0) without (c) or with (d) increasing amounts of NaCN (1−100 μM) and dilution with dichloroethane (120 μL).

the absorption spectra of acetonitrile solutions of **7a** do not show any increase in absorbance in the visible region even after the addition of sodium phosphate buffer containing large amounts (10 mM) of NaF (c in Figure 11), NaCl (d), NaBr (e), or NaI (f).

Acetonitrile solutions of **7a** respond to aqueous solutions of cyanide with a detectable absorbance change only if the cyanide concentration is greater than 0.1 mM. The chromogenic response, however, improves considerably when **7a** is dissolved in dichloroethane together with Bu_4NCl. The resulting organic solutions change color when treated with aqueous solutions containing micromolar concentrations of cyanide (a−c in Figure 12). Presumably, the tetrabutylammonium salt facilitates the

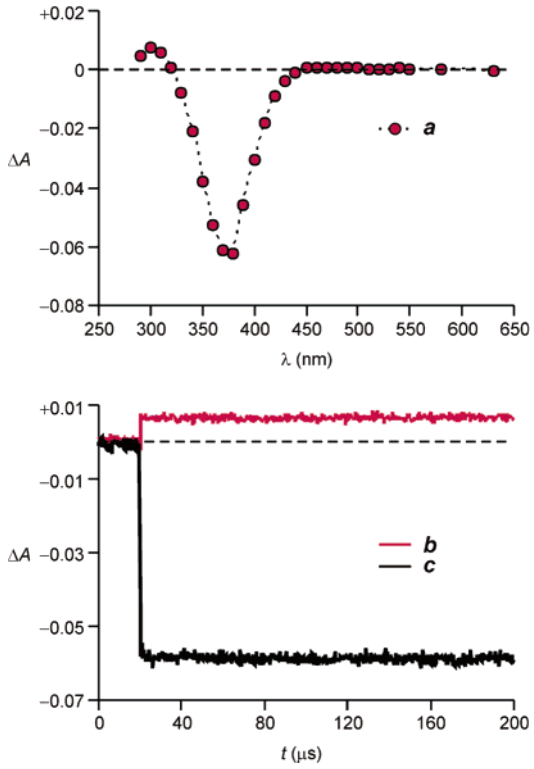

FIGURE 14. Transient absorption spectrum (a) of **8a** recorded 4 μs after the laser pulse (355 nm, 6 ns, 8 mJ, 0.1 mM, MeCN, 295 K) and evolution of the absorbance at 290 (b) and 380 (c) nm upon laser excitation.

transfer of cyanide anions from the aqueous to the organic phase and encourages the chromogenic transformation. Furthermore, the chromogenic process is particularly sensitive to the pH of the aqueous phase and has an optimal response to cyanide at a pH of 9.0. Indeed, the absorbance of the organic solution at 581 nm remains negligible up to this particular pH value (a in Figure 13) in the absence of cyanide salts in the aqueous phase. Instead, the absorbance increases significantly with the pH of the aqueous solution when this particular phase contains cyanide anions (b in Figure 13). At a pH of 9.0, even micromolar concentrations of cyanide in the aqueous phase are sufficient to impose a detectable change on the absorbance of the organic phase (c and d in Figure 13).

Transient Absorption Spectroscopy. The laser excitation of the [1,3]oxazine **1a** induces the formation of the ring-opened isomer **1b** in less than 6 ns with a quantum yield of 0.1 in aerated acetonitrile.[38] The photogenerated species reverts to the original form with a lifetime of 22 ns. In principle, a similar process can also occur upon excitation of the [1,3]oxazines **7a** and **8a**. To explore this possibility, we have analyzed **8a** by laser flash photolysis. In contrast to the behavior of **1a**, the characteristic absorption of **8b** cannot be detected in the resulting transient absorption spectra. Instead, an increase in absorbance at 290 nm and the bleaching of the $\pi \rightarrow \pi^*$ transition of the 4-nitrophenylazophenyl chromophore at 380 nm are evident in the spectrum recorded after 4 μs from the laser pulse (a in Figure 14). Both transient bands remain constant in the microsecond domain (b and c in Figure 14), but eventually disappear with millisecond−second time scales.[42] In fact, the steady-state absorption spectra recorded before and after the laser flash photolysis experiment are virtually indistinguishable. These observations are consistent with the photoinduced trans → cis

isomerization of the 4-nitrophenylazophenyl chromophore of **8a**, followed by the thermal cis → trans re-isomerization, and exclude the photoinduced ring opening observed for **1a**.

Conclusions

The cyanide anion can be detected colorimetrically relying on the opening of a [1,3]oxazine ring and the concomitant formation of a 4-nitrophenylazophenolate chromophore. Chromogenic molecules able to satisfy these design requirements can be prepared by fusing a benzooxazine ring to an indoline fragment. The [1,3]oxazine ring of the resulting compounds opens and closes rapidly on the ^{1}H NMR time scale in acetonitrile-d_3 at ambient temperature. The free energy barrier for the ring-opening process increases when either (1) the substituent on the carbon atom at the junction of the two heterocycles changes from a methyl to a phenyl group or (2) the solvent varies from acetonitrile-d_3 to toluene-d_8. The ring-opened isomer is short-lived, but can be trapped with the addition of a nucleophile. For example, a cyanide anion can attack the electrophilic indolium cation of this species preventing the ring-closing process. The result is the quantitative formation of a cyanoamine and the appearance of an intense band in the visible region of the absorption spectrum, corresponding to a 4-nitrophenylazophenolate chromophore. The chromogenic response of the phenyl-substituted oxazine to cyanide requires several minutes to reach a steady state. Instead, the coloration of the methyl-substituted oxazine occurs on a time scale of seconds. Furthermore, this particular compound is not affected by fluoride, chloride, bromide, and iodide anions, which are common interferents in conventional sensing schemes for cyanide.[32−37] Finally, dichloroethane solutions of this oxazine and a phase-transfer catalyst respond to aqueous solutions containing micromolar amounts of cyanide with a noticeable absorbance increase in the visible region, offering detection limits comparable to those of the best chemosensors available for this anion.[36,37] Thus, our operating principles for the colorimetric detection of cyanide can eventually evolve into fast and simple assays for the determination of relatively small amounts of this toxic analyte in water without suffering from the deleterious interference of common anions.

Experimental Section

2-Hydroxymethyl-4-(4′-nitrophenylazo)phenol (4). A solution of **3** (1.12 g, 5 mmol) in H_2O (15 mL) was added over 90 min to a solution of **2** (535 mg, 4.3 mmol) in aqueous NaOH (1 M, 5 mL) and H_2O (10 mL) maintained at 0 °C. The mixture was stirred for a further 45 min. During this time, the temperature was allowed to raise to ambient conditions and the pH was maintained at ca. 8 by adding aliquots of aqueous NaOH (1 M). After the addition of aqueous HCl (1 M, 5 mL), the mixture was cooled to −5 °C and maintained at this temperature for 1 h. The resulting precipitate was filtered, dissolved in $MeCO_2Et$ (50 mL), and dried ($MgSO_4$). After filtration, the solvent was distilled off under reduced pressure to afford **4** (1.13 g, 96%) as a bright-orange solid. Mp 178−179 °C; FABMS *m*/*z* 274 $[M + H]^+$; ^{1}H NMR (500 MHz, chloroform-*d*) δ 2.43 (1H, br s), 5.03 (2H, s), 7.05 (1H, d, J = 9 Hz), 7.73 (1H, d, J = 2 Hz), 7.85 (1H, dd, J = 2 and 9 Hz), 7.97 (2H, d, J = 9 Hz), 8.15 (1H, br s), 8.36 (2H, d, J = 9 Hz); ^{13}C NMR (100 MHz, chloroform-*d*) δ 60.4, 116.3, 123.3, 123.8, 125.6, 125.7, 130.4, 147.1, 149.1, 157.1, 160.4.

2-(4′-Nitrophenylazo)-5a,6,6-trimethyl-5a,6-dihydro-12H-indolo[2,1-b][1,3]benzooxazine (7a). A solution of PBr_3 in CH_2Cl_2 (1:20 v/v, 360 μL) was added over 20 min to a solution of **4** (117 mg, 0.4 mmol) in CH_2Cl_2 (25 mL) maintained at 0 °C under N_2. The mixture was stirred for a further 3 h. During this time, the temperature was allowed to raise to ambient conditions. At this point, **5** (345 μL, 2 mmol) was added and the mixture was stirred for a further 1 h. After filtration over a plug of SiO_2, the solvent was distilled off under reduced pressure and the residue was purified by HPLC [semipreparative, MeCN/H_2O (95:5 v/v)] to give **7a** (73 mg, 41%) as an orange-red solid. HPLC [analytical, MeCN/H_2O (90:10 v/v)] RT = 4.1 min, PA = 1.4, APP = 310.4 ± 1.3 nm; mp 156 °C; FABMS *m*/*z* 415 $[M + H]^+$; ^{1}H NMR (500 MHz, chloroform-*d*) δ 1.25 (3H, s), 1.51 (3H, s), 1.61 (3H, s), 4.66 (2H, s), 6.59 (1H, d, J = 8 Hz), 6.80 (1H, d, J = 9 Hz), 6.82 (1H, t, J = 7 Hz), 7.08 (1H, td, J = 1 and 8 Hz), 7.13 (1H, dd, J = 1 and 7 Hz), 7.74 (1H, dd, J = 2 and 9 Hz), 7.80 (1H, d, J = 2 Hz), 7.96 (2H, d, J = 9 Hz), 8.37 (2H, d, J = 9 Hz); ^{13}C NMR (100 MHz, chloroform-*d*) δ 16.7, 19.1, 26.2, 40.5, 48.2, 103.8, 108.6, 118.8, 119.4, 120.4, 121.5, 122.4, 122.7, 123.3, 124.9, 127.7, 138.4, 146.4, 147.4, 148.6, 156.5, 158.1.

2-(4′-Nitrophenylazo)-5a-phenyl-6,6-dimethyl-5a,6-dihydro-12H-indolo[2,1-b][1,3]benzooxazine (8a). A solution of PBr_3 in MeCN (1:10 v/v, 190 μL) was added over 20 min to a solution of **4** (185 mg, 0.6 mmol) in MeCN (25 mL) maintained at 0 °C under Ar. After addition of Et_3N (80 μL), the mixture was stirred for a further 1 h at 0 °C and then heated under reflux for 4 h. At this point, **6** (400 mg, 1.8 mmol) was added and the temperature was allowed to lower to ambient conditions. After 36 h, the solvent was distilled off under reduced pressure and the residue was purified by column chromatography [SiO_2, hexane/CH_2Cl_2 (1:1 v/v)] to give **8a** (135 mg, 51%) as an orange-red solid. HPLC [analytical, MeCN/H_2O (90:10 v/v)] RT = 4.1 min, PA = 1.6, APP = 303.2 ± 1.0 nm; mp 200 °C; FABMS *m*/*z* 476 $[M]^+$; ^{1}H NMR (400 MHz, chloroform-*d*) δ 0.85 (3H, s), 1.60 (3H, s), 4.57 (1H, d, J = 11 Hz), 4.67 (1H, d, J = 11 Hz), 6.75 (1H, d, J = 8 Hz), 6.90 (1H, t, J = 7 Hz), 6.97 (1H, d, J = 9 Hz), 7.16−7.19 (2H, m), 7.35−7.42 (3H, m), 7.64−7.73 (4H, m), 7.93 (2H, d, J = 9 Hz), 8.34 (2H, d, J = 9 Hz); ^{13}C NMR (100 MHz, chloroform-*d*) δ 22.9, 31.8, 41.2, 49.8, 104.8, 109.2, 118.7, 120.6, 120.7, 122.4, 122.6, 123.3, 124.3, 124.9, 127.8, 128.3, 128.7, 129.0, 137.0, 138.0, 146.6, 147.5, 148.4, 156.2, 157.9.

X-ray Crystallography. Single crystals of **1d** were grown from an equimolar solution of **1a** and Bu_4NCN in chloroform/hexane (2:1 v/v) maintained in the refrigerator. Single crystals of **7a** and **8a** were grown by vapor diffusion of MeOH into a solution of the corresponding compound in chloroform/hexane (2:3 v/v for **7a** and 2:1 v/v for **8a**).

Crystal data for 1d: $[C_{24}H_{20}N_3O_3](C_{16}H_{36}N)\cdot 3H_2O$, M = 694.94, monoclinic, $P2_1/n$ (no. 14), a = 9.5783(9) Å, b = 25.749(3) Å, c = 16.5586(17) Å, β = 96.163(8)°, V = 4060.3(7) Å^3, Z = 4, D_c = 1.137 g cm^{-3}, μ(Cu Kα) = 0.606 mm^{-1}, T = 173 K, yellow/brown needles; 7678 independent measured reflections, F^2 refinement, R_1 = 0.103, wR_2 = 0.159, 5514 independent observed absorption-corrected reflections [$|F_o| > 4\sigma(|F_o|)$, $2\theta_{max}$ = 142°], 468 parameters. CCDC 283555.

Crystal data for 7a: $C_{24}H_{22}N_4O_3$, M = 414.46, monoclinic, $P2_1/c$ (no. 14), a = 22.661(4) Å, b = 14.4660(18) Å, c = 13.077(6) Å, β = 102.33(3)°, V = 4188(2) Å^3, Z = 8 (two independent molecules), D_c = 1.315 g cm^{-3}, μ(Mo Kα) = 0.089 mm^{-1}, T = 203 K, orange platy needles; 7353 independent measured reflections, F^2 refinement, R_1 = 0.064, wR_2 = 0.127, 3957 independent observed reflections [$|F_o| > 4\sigma(|F_o|)$, $2\theta_{max}$ = 50°], 560 parameters. CCDC 261143.

Crystal data for 8a: $C_{29}H_{24}N_4O_3$, M = 476.52, monoclinic, $P2_1/c$ (no. 14), a = 8.7976(12) Å, b = 18.011(6) Å, c = 15.680(4) Å, β = 104.74(2)°, V = 2402.7(10) Å^3, Z = 4, D_c = 1.317 g cm^{-3}, μ(Cu Kα) = 0.704 mm^{-1}, T = 293 K, orange/yellow blocks; 3566 independent measured reflections, F^2 refinement, R_1 = 0.060,

(42) The transient absorption spectra of **8a** trapped in poly(methyl methacrylate) matrixes show essentially the same temporal evolution (Figure S16).

$wR_2 = 0.168$, 2719 independent observed reflections [$|F_o| > 4\sigma(|F_o|)$, $2\theta_{max} = 120°$], 314 parameters. CCDC 261144.

Absorption Spectroscopy. The steady-state spectra were recorded in aerated MeCN, using quartz cells with a path length of 0.5 cm. The transient spectra were recorded either in aerated MeCN, using quartz cells with a path length of 1.0 cm, or in poly(methyl methacrylate) (PMMA). The excitation source was a Nd:YAG laser (355 nm, 6 ns, 8 mJ). The PMMA films were prepared by spin-coating aliquots of CH_2Cl_2 solutions of the polymer (160 mg mL^{-1}) and **8a** (8 mg mL^{-1}) on glass plates at 420 rpm for 9 s. The thickness of the resulting films (ca. 6 μm) was measured with a digital micrometer.

Acknowledgment. We thank the National Science Foundation (CAREER Award CHE-0237578), University of Miami, and MIUR (Rome, Italy) for financial support.

Supporting Information Available: General methods and experimental procedures for the synthesis of **11**; high-performance liquid chromatograms of **7a** and **8a**; single-crystal X-ray structures of **1d**, **7a**, and **8a**; partial ^{1}H NMR spectra of **8a** at various temperatures; partial ^{1}H NMR spectra of **7a** and **8a** before and after the addition of Bu_4NOH; partial ^{1}H NMR spectra of **8a** before and after the addition of Bu_4NCN; steady-state absorption spectra of **8a** before and after the addition of Bu_4NOH; steady-state absorption spectra of **8a** before and after the addition of Bu_4NCN; kinetic trace for **8a** in poly(methyl methacrylate) upon laser excitation. This material is available free of charge via the Internet at http://pubs.acs.org.

JO052096R